Angewandte
Eine Zeitschrift der Gesellschaft Deutscher Chemiker
Chemie

Supporting Information

Coupling of the Decarboxylation of 2-Cyano-2-phenylpropanoic Acid to Large-Amplitude Motions: A Convenient Fuel for an Acid–Base-Operated Molecular Switch

*José Augusto Berrocal, Chiara Biagini, Luigi Mandolini, and Stefano Di Stefano**

anie_201602594_sm_miscellaneous_information.pdf

INDEX

	Page
Instruments, methods and materials and decarboxylation procedures	S2
1D NMR characterization of **3•H$^+$** and **3•(H$_2$)$^{2+}$**	S4
^{1}H NMR and ^{13}C NMR spectra of **3•H$^+$**	S5
^{1}H NMR and ^{13}C NMR spectra of **[3•(H$_2$)]$^{2+}$**	S7
2D NMR characterization of **3•H$^+$** and **3•(H$_2$)$^{2+}$**	S9
Comparison of ^{1}H NMR spectra of **3**, **3•H$^+$**, **3•Cu$^+$** and **[3•(H)$_2$]$^{2+}$** with assignments	S17
Zoom-in of the double bond region of Figure S7	S18
^{1}H NMR titration of $Bu_2NH_2PF_6$ with **3**	S19
UV-vis titration of **3** with $Bu_2NH_2PF_6$	S19
Decarboxylation of acid **1** in the presence of stoichiometric (1:1) and substoichiometric (1:0.5) amounts of Et_3N	S20
^{1}H NMR monitoring of reactions between **1** (5 mM) and **3** (5 mM)	S23
^{1}H NMR monitoring of reactions between **1** (10 mM) and **3** (10 mM)	S24
^{1}H NMR monitoring of reactions between **1** (4 mM) and **3** (2 mM)	S25
^{1}H NMR monitoring of reactions between **1** (5 mM) and **3** (0.5 mM)	S26

Instruments and Methods

^{1}H NMR spectra were recorded on a 300 MHz spectrometer. The spectra were internally referenced to the residual proton solvent signal.

Materials

All reagents and solvents were purchased at the highest commercial quality and were used without further purification, unless otherwise stated. CD_2Cl_2 was flashed through basic alumina (4 Å) immediately prior to use. Acid **1** was prepared according to a literature procedure.[S1] Spectroscopic data of acid **1** were in agreement with literature data. Catenand **3** was available from a previous investigation.[S2] Et_3N was distilled from metallic sodium before use.

Decarboxylaton Procedures

*Procedure for decarboxylation of acid **1** (10 mM) in presence of Et_3N (10 mM)*

Acid **1** (1.05 mg, 6 µmol) was weighed in a NMR tube and CD_2Cl_2 (570 µL) previously flashed through basic alumina was added. To such solution, 30 µL of a 0.20 M stock solution of Et_3N in CD_2Cl_2 were added. Reaction progress was monitored by ^{1}H-NMR spectroscopy (probe thermostated at 25°C).

*Procedure for decarboxylation of acid **1** (10 mM) in presence of Et_3N (5 mM)*

Acid **1** (1.05 mg, 6 µmol) was weighed in a NMR tube and CD_2Cl_2 (570 µL) previously flashed through basic alumina was added. To such solution, 30 µL of a 0.10 M stock solution of Et_3N in CD_2Cl_2 were added. Reaction progress was monitored by ^{1}H-NMR spectroscopy (probe thermostated at 25°C).

[S1] Brunner, H.; Schmidt, P. *Eur. J. Org. Chem.* **2000**, 2119-2133.

[S2] a) Berrocal, J. A.; Nieuwenhuizen, M. M. L.; Mandolini, L.; Meijer, E. W.; Di Stefano, S. *Org. Biomol. Chem.* **2014**, *12*, 6167-6174.

*Procedure for decarboxylation of acid **1** (5 mM) in presence of catenand **3** (5 mM)*

Catenand **3** (2.90 mg, 3 μmol) was weighed in a NMR tube and CD_2Cl_2 (570 μL) previously flashed through basic alumina was added. To such solution, 30 μL of a 0.10 M stock solution of acid **1** in CD_2Cl_2 were added. Reaction progress was monitored by ^{1}H-NMR spectroscopy (probe thermostated at 25°C).

*Procedure for decarboxylation of acid **1** (10 mM) in presence of catenand **3** (10 mM)*

Catenand **3** (5.80 mg, 6 μmol) was weighed in a NMR tube and CD_2Cl_2 (570 μl) previously flashed through basic alumina was added. To such solution, 30 μl of a 0.20 M stock solution of acid **1** in CD_2Cl_2 were added. Reaction progress was monitored by ^{1}H-NMR spectroscopy (probe thermostated at 25°C).

*Procedure for decarboxylation of acid **1** (4 mM) in presence of catenand **3** (2 mM)*

Catenand **3** (1.16 mg, 1.20 μmoL) was weighed in a NMR tube and CD_2Cl_2 (570 μL) previously flashed through basic alumina was added. To such solution, 30 μL of a 0.080 M stock solution of acid **1** in CD_2Cl_2 were added. Reaction progress was monitored by ^{1}H-NMR spectroscopy (probe thermostated at 25°C).

*Procedure for decarboxylation of acid **1** (5 mM) in presence of catenand **3** (0.5 mM)*

Catenand **3** (0.29 mg, 0.3 μmol) was weighed in a NMR tube and CD_2Cl_2 (570 μL) previously flashed through basic alumina was added. To such solution, 30 μL of a 0.10 M stock solution of acid **1** in CD_2Cl_2 were added. Reaction progress was monitored by ^{1}H-NMR spectroscopy (probe thermostated at 25°C).

*Procedure for decarboxylation of acid **1** (5 mM) in presence of Proton Sponge (5 mM)*

Acid **1** (0.53 mg, 3 μmol) was weighed in a NMR tube and CD_2Cl_2 (570 μL) previously flashed through basic alumina were added. To such solution, 30 μL of a 0.10 M stock solution of Proton Sponge in CD_2Cl_2 were added. Reaction runs were monitored by ^{1}H-NMR spectroscopy (probe thermostated at 25°C).

Compounds characterization

3•H$^+$ (mixture of EE, ZZ and EZ isomers)

^{1}H NMR (400 MHz, CD_2Cl_2, signals of the most abundant isomer are reported) δ: 8.52 (d, J = 8 Hz, 4H), 8.03 (s, 4H), 7.69 (d, J = 8 Hz, 4H), 5.70-5.68 (m, 4H), 2.53-2.48 (m, 8H), 2.14 (q, J = 8 Hz, 8H) 1.50-1.42 (m, 8H), 1.35-1.29 (m, 8H), 1.13-1.01 (m, 16H), 0.81-0.69 (m, 16H), 0.60-0.52 (m, 8H), 0.24-0.16 (m, 8H).

^{13}C NMR (100 MHz, CD_2Cl_2) δ: 163.21, 141.78, 139.56, 131.28, 130.46, 128.54, 127.09, 124.98, 37.81, 37.53, 33.44, 31.03, 30.85, 30.74, 30.71, 30.53, 30.26, 30.16, 30.07, 30.02, 29.87, 29.86, 29.77, 29.73, 29.68, 29.39, 29.33, 28.47.

HRMS-MALDI TOF(m/z): [M + H$^+$] calcd for $C_{68}H_{97}N_4$, 969.7713; found, 969.7747

[3•(H_2)]$^{2+}$ (mixture of EE, ZZ and EZ isomers)

^{1}H NMR (400 MHz, CD_2Cl_2, signals of the most abundant isomer are reported) δ: 8.69 (d, J = 8 Hz, 4H), 8.10 (s, 4H), 7.90 (d, J = 8 Hz, 4H), 5.48-5.45 (m, 4H), 3.31-2.98 (m, 8H), 2.02-1.92 (m, 8H), 1.79-1.59 (m, 8H), 1.34-1.13 (m, 56H).

^{13}C NMR (100 MHz, CD_2Cl_2) δ: 163.27, 163.17, 130.99, 130.47, 128.72, 127.28, 125.97, 117.41, 114.54, 37.95, 37.69, 33.34, 30.98, 30.85, 30.59, 30.45, 30.25, 30.02, 29.99, 29.88, 29.81, 29.71, 29.66, 29.54, 29.50, 28.47.

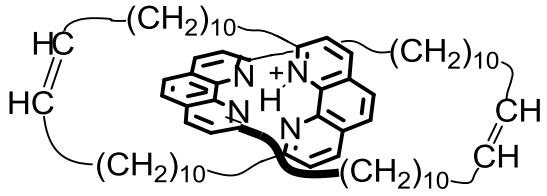
HC
(CH2)10
(CH2)10
HC
N
+N
H
N
N
CH
CH
(CH2)10
(CH2)10
CF3CO2−

3•H^+

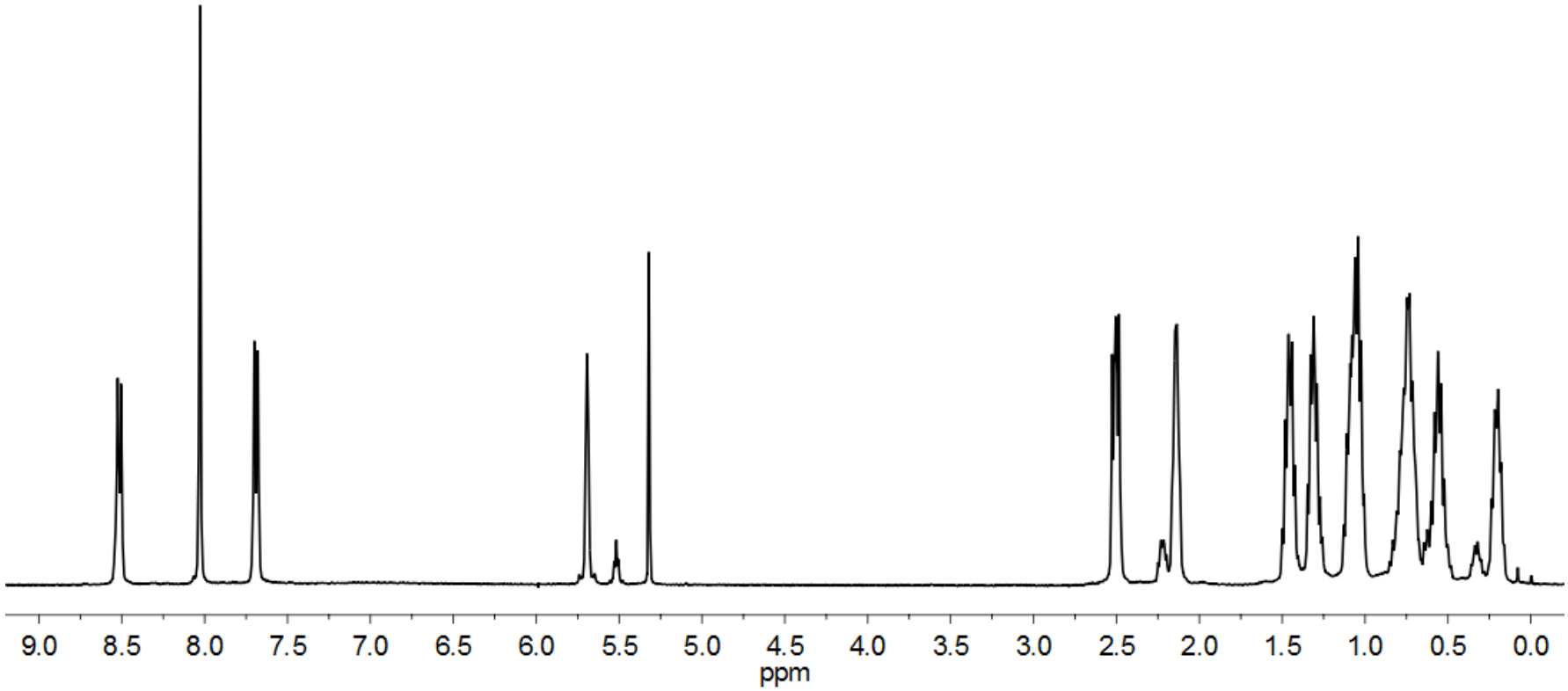
9.0
8.5
8.0
7.5
7.0
6.5
6.0
5.5
5.0
4.5
4.0
3.5
3.0
2.5
2.0
1.5
1.0
0.5
0.0
ppm

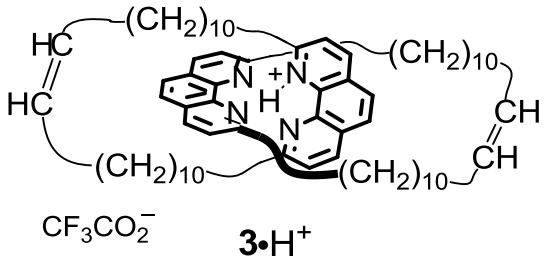
(CH2)10
HC
HC
(CH2)10
(CH2)10
CH
CH
(CH2)10
N
+
H
N
N
N
CF3CO2−

3•H$^+$

170
160
150
140
130
120
110
100
90
80
70
60
50
40
30
20
10
0
ppm

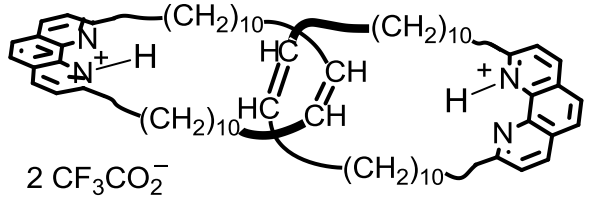

$[\mathbf{3}\bullet(H)_2]^{2+}$

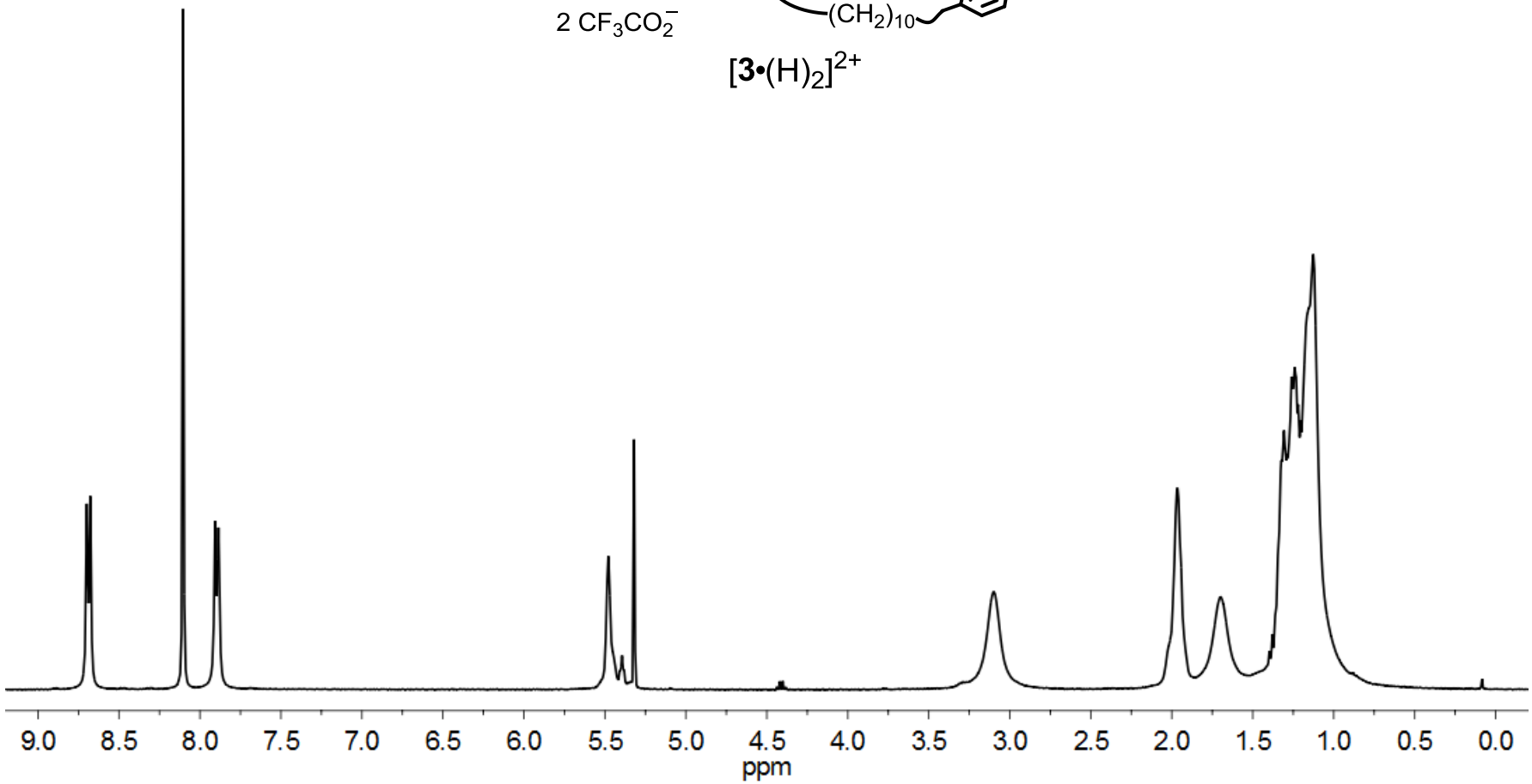

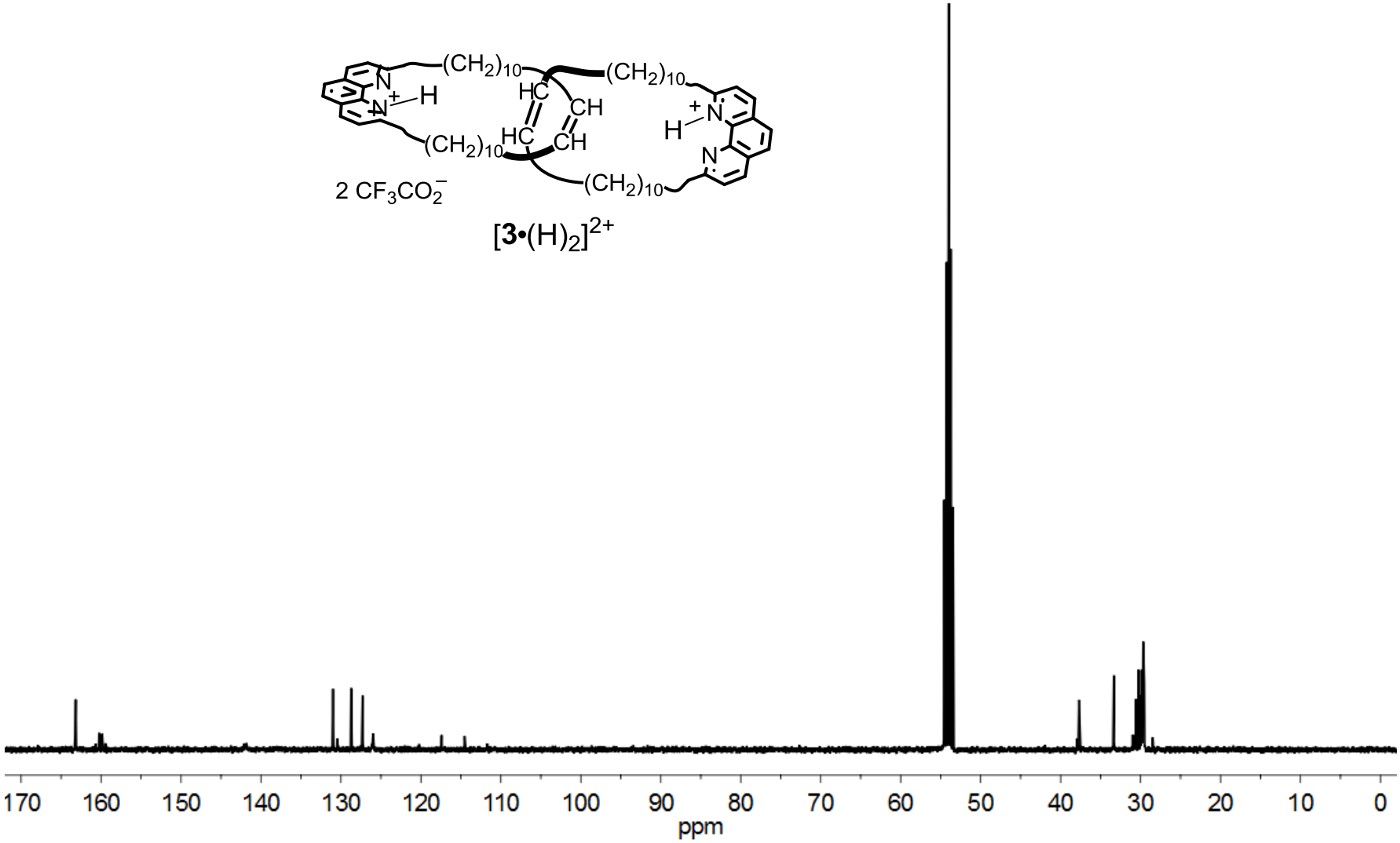
(CH2)10
(CH2)10
HC
CH
HC
CH
(CH2)10
(CH2)10
N
H
N
H
N
2 CF3CO2−
170
160
150
140
130
120
110
100
90
80
70
60
50
40
30
20
10
0
ppm

[**3**•$(H)_2$]$^{2+}$

2D NMR characterization of **3•H$^+$** and **[3•(H$_2$)]$^{2+}$**

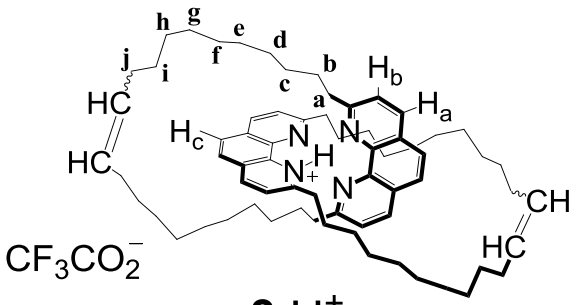

3•H$^+$

Full assignment of all chain methylene proton signals of **3•H$^+$** was performed with a 2D-COSY (Figure S1 and S2) experiment. Starting from either the signals of the double bond protons or the first methylene protons **a**, the cross correlation signals allow to track the connectivity of the sets **j**-**g** and **a**-**f** (Figure S2). Comparison with the previously assigned signals[S2] of methylene protons of **3•Cu$^+$** shows similar displacements after complexation/protonation of catenand **3** (Figure S7).

The structure of **3•H$^+$** was also studied with 2D-ROESY. The following ROE interactions are seen: protons H_c with protons **d**, **e**, **f**, **g**, **h**, **i**, **j**; protons H_c with double bond protons; protons H_a with protons **e**, **f**, **g**, **h** and **i**. The same ROE interactions were found for **3•Cu$^+$**.[S2]

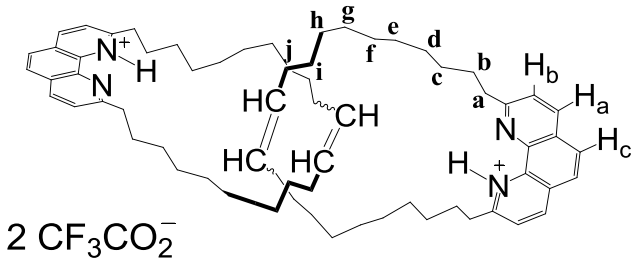

[3•(H$_2$)]$^{2+}$

The 2D-COSY NMR spectrum of **[3•(H$_2$)]$^{2+}$** (Figure S5) is little informative of the connectivity of the alkyl chains because of overlap of many methylene signals (again, the signal of the double bond and methylene **a** allow to track methylenes **j** and **b)**. In any event, we note that the 2D-COSY spectrum **[3•(H$_2$)]$^{2+}$** is very similar to that of **3**.[S2]

As to the 2D-ROESY spectrum of **[3•(H_2)]$^{2+}$** (Figure S6) no ROE interactions are found between aromatic protons and the methylene groups, as well as between the same aromatic protons and the double bond protons, apart from the obvious interactions of H_b with methylenes **a** and **b**. Once again, a similar situation was observed in the corresponding spectrum of **3**.[S2] Therefore, it appears most likely that in both **3** and **3**•(H^+)$_2$ the contact between the interlocked rings involves the double bond regions, with the advantage that repulsive interactions between the hydrogen atoms of the CH_2 groups belonging to one ring with those belonging to the other are avoided, or at least minimized. This situation is strongly reminiscent of that found in the medium rings, in which a major source of strain is the transannular repulsion of the CH_2 groups. A significant strain relief is obtained by replacement of such groups by heteroatoms or trigonal carbon atoms. For example, the strain energies of *cis*-cyclodecene and *cis*,*cis*-1,6-cyclodecadiene are 5.41 and 9.66 kcal mol^{-1} lower than that of cyclodecane (data from N. L. Allinger, J. T. Sprague, *J. Am. Chem. Soc.* **1972**, *95*, 5743-5747).

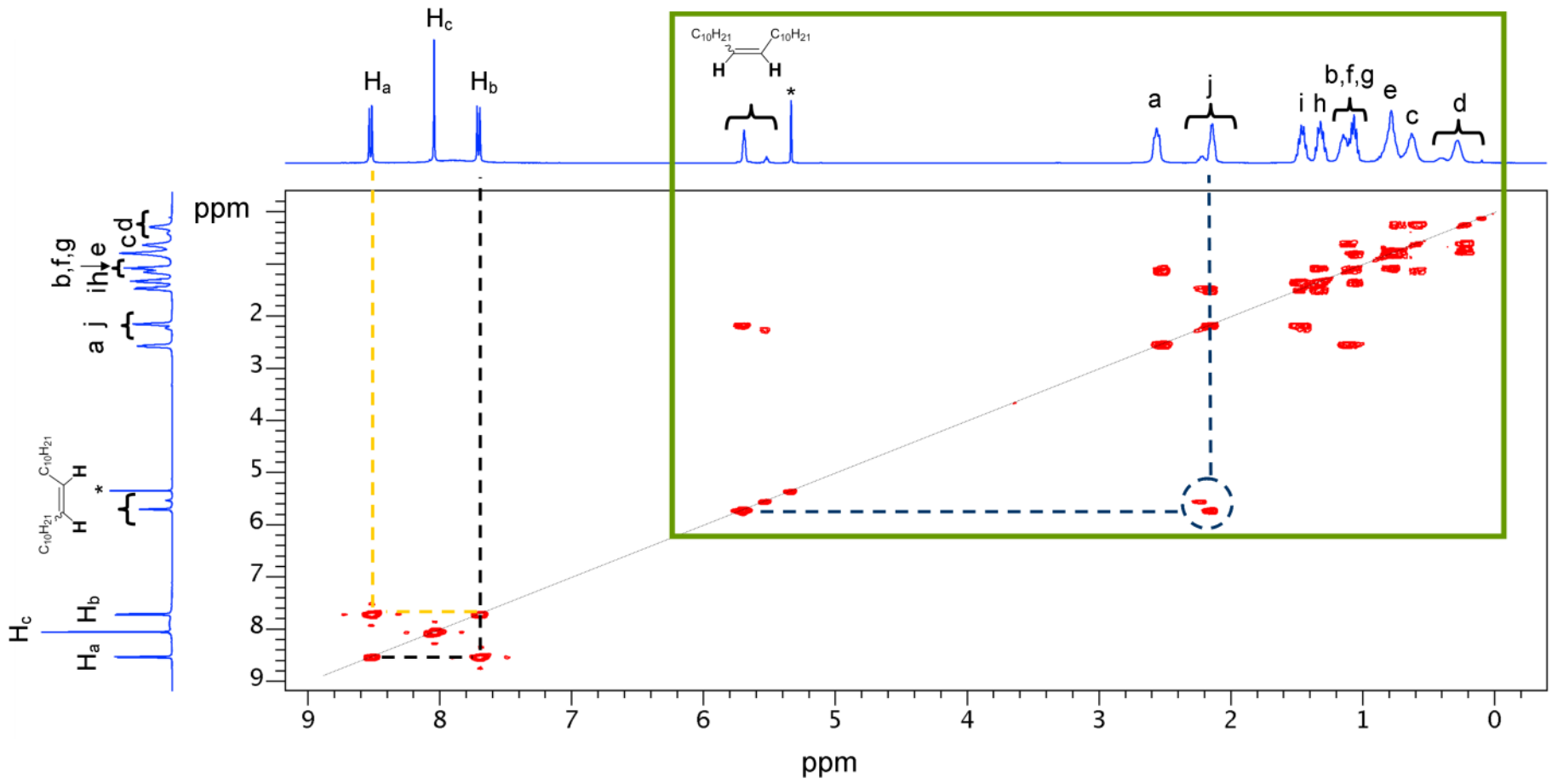

Figure S1. Full 2D COSY spectrum of **3•H$^+$**. Correlations between aromatic protons H_a and H_b and the double bond protons and protons **j** are shown with dashed lines. The green box highlights the aliphatic region, which is expanded and analyzed in Figure S2.

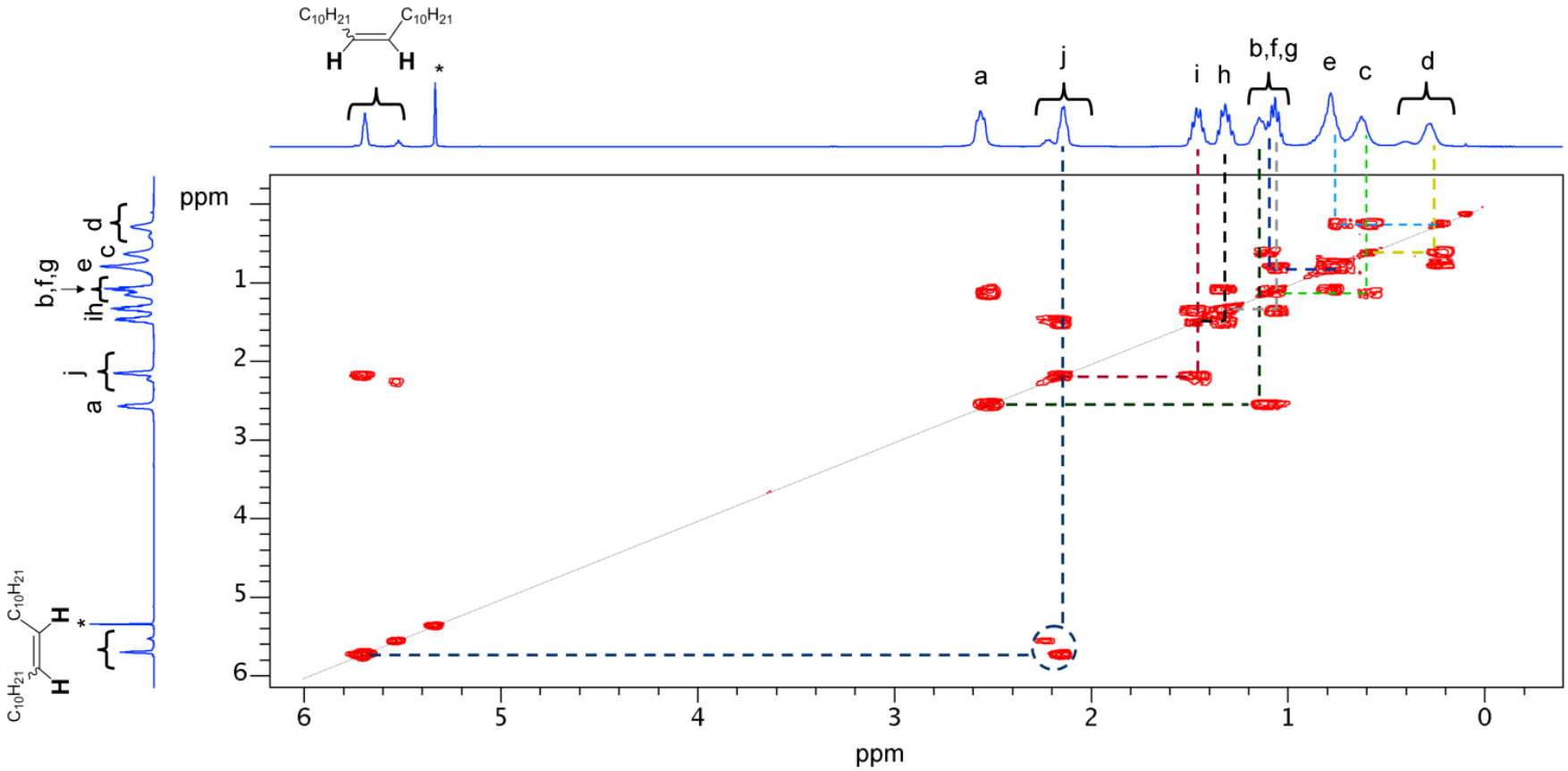

Figure S2. Expansion of the 2D COSY spectrum of **3•H**$^{+}$ shown in Figure S1, featuring only the aliphatic signals. Out of diagonal correlations between methylene protons are shown with colored dashed lines.

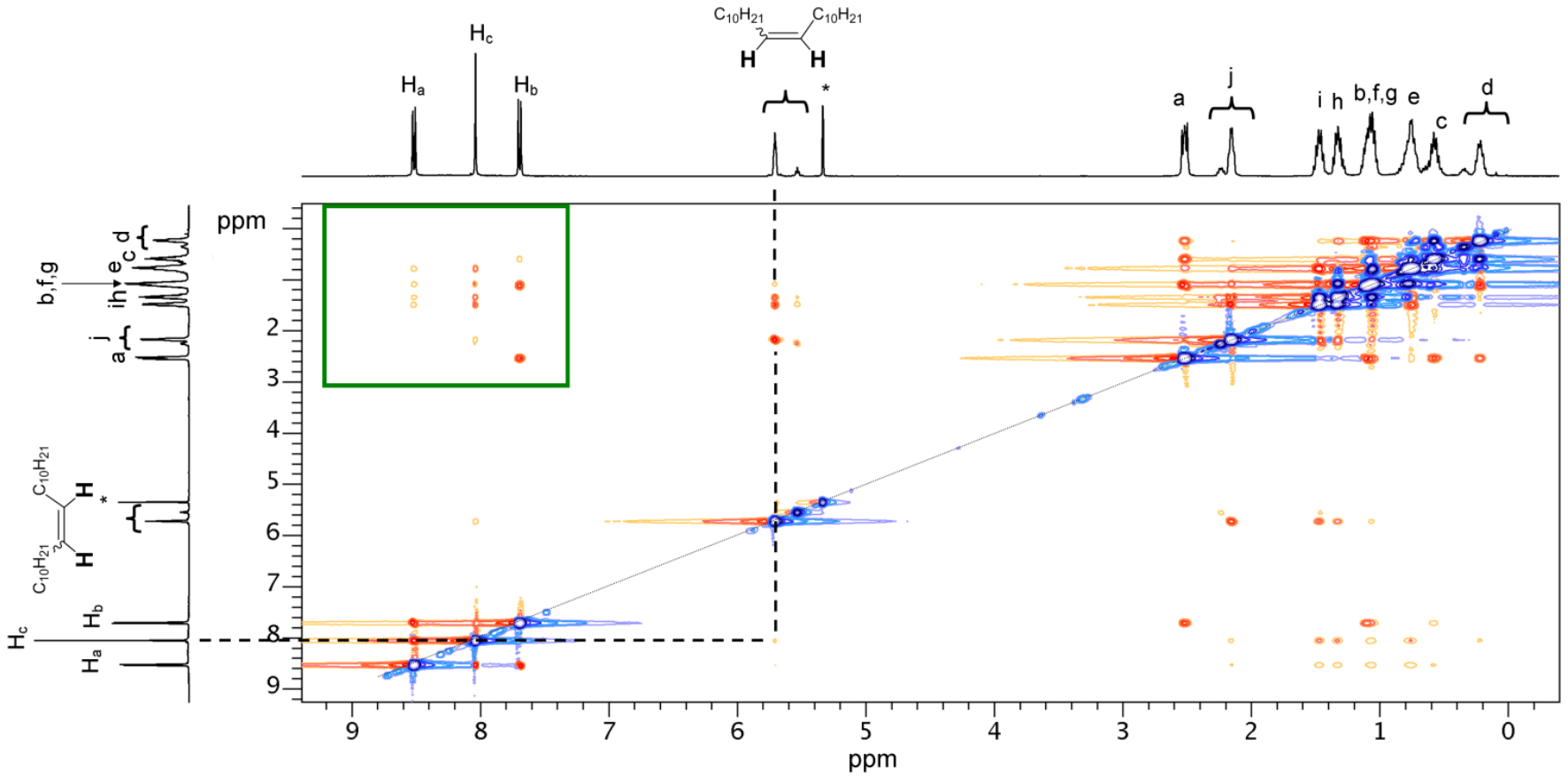

Figure S3. Full 2D ROESY spectrum of **3•H$^+$**. Correlation between aromatic protons H_c and the double bond protons is shown with dashed lines. The green box highlights the out of diagonal correlation signals between methylene and aromatic protons. This part of the spectrum is expanded and analyzed in Figure S4.

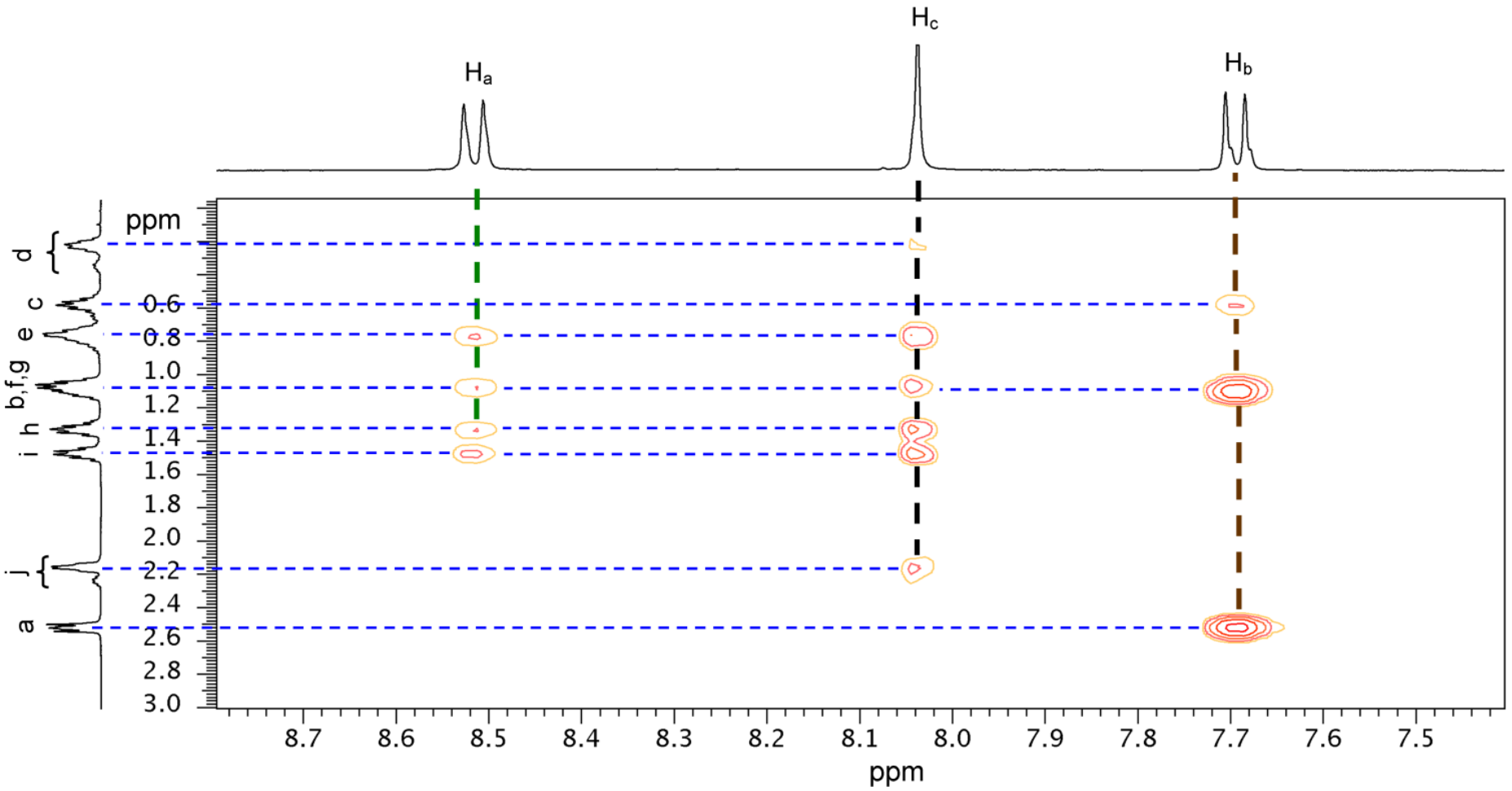

Figure S4. Expansion of the 2D ROESY spectrum of **3•H$^+$** shown in Figure S3, showing ROE interactions between aliphatic and aromatic signals. Some methylene protons show ROE interactions with more than one aromatic singal, therefore dashed vertical lines posses different colors to distinguish the aromatic nuclei, whereas horizontal dashed lines are all blue.

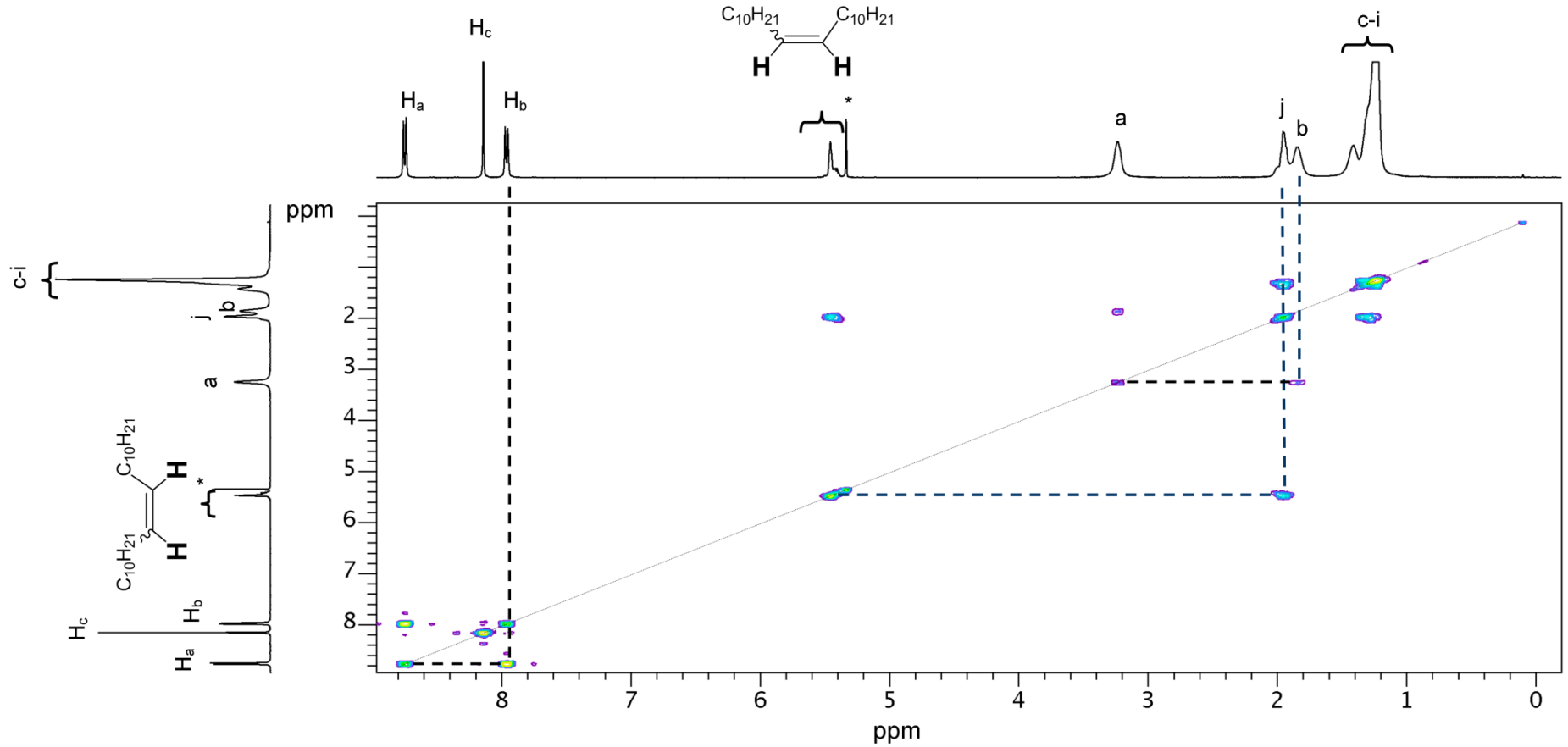

Figure S5. Full 2D COSY spectrum of **[3•(H)$_2$]$^{2+}$**. The spectrum only shows correlations between aromatic protons H_a and H_b, double bond protons and methylene protons **j**, and methylene protons **a** and **b**. Out of diagonal correlations are all highlighted with dashed lines.

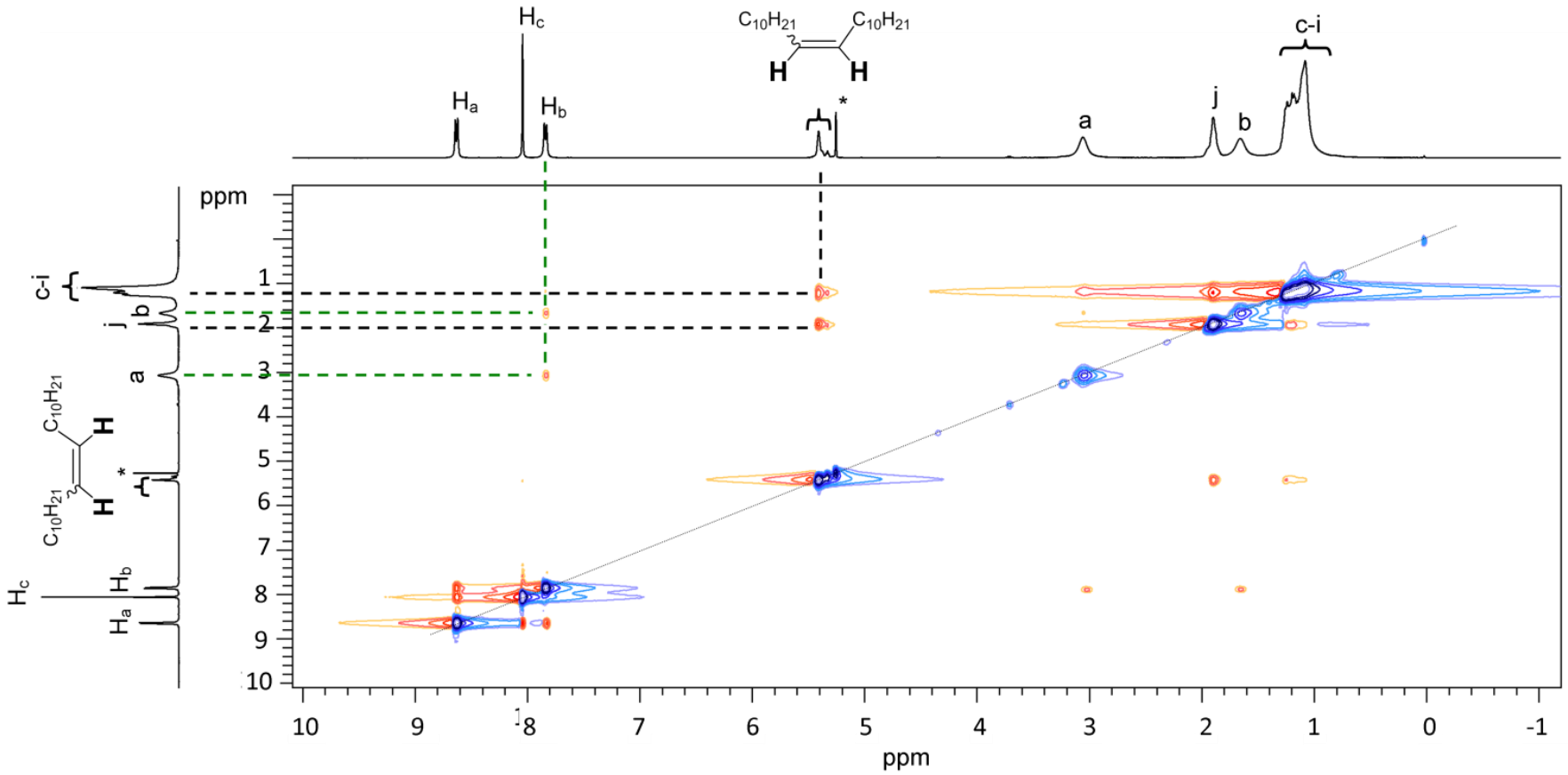

Figure S6. Full 2D ROESY spectrum of **[3•(H)$_2$]$^{2+}$**. The spectrum only shows correlations between aromatic protons H_b and methylene protons **a** and **b**, and double bond protons with methylene proton **j** and, most likely, **i**. Correlations are all highlighted with dashed lines.

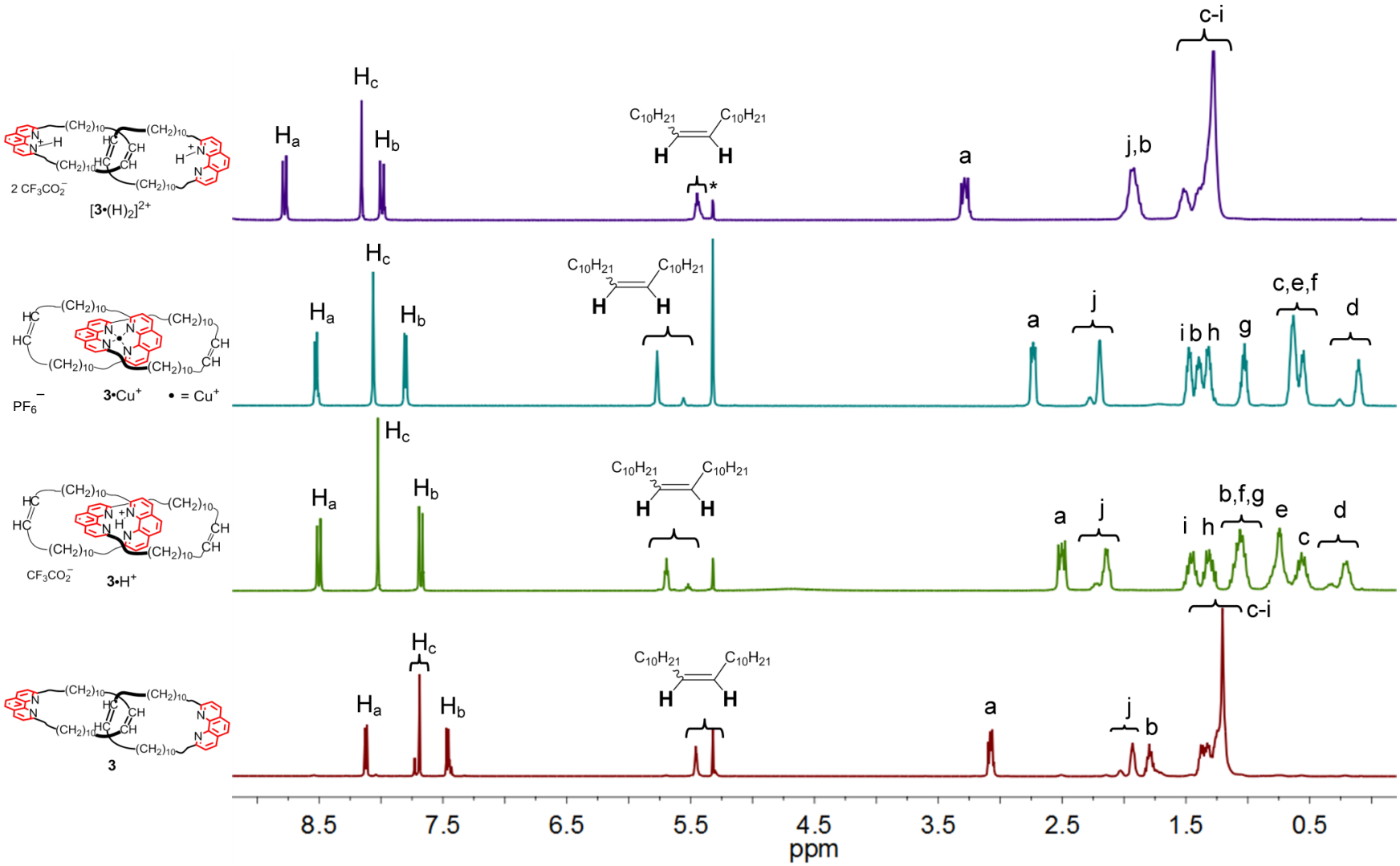

Figure S7. Comparison of ^{1}H NMR spectra of **3**, **3•H^{+}**, **3•Cu^{+}** and **[3•(H)$_2$]$^{2+}$**, with assigned peaks. Assignment for **3** and **3•Cu^{+}** was already known.[S2] Assignment for **3•H^{+}** and **[3•(H)$_2$]$^{2+}$** has been carried out on the basis of the 2D NMR spectra in previous pages. See page S9 for labeling. The asterisk denotes the peak of $CHDCl_2$.

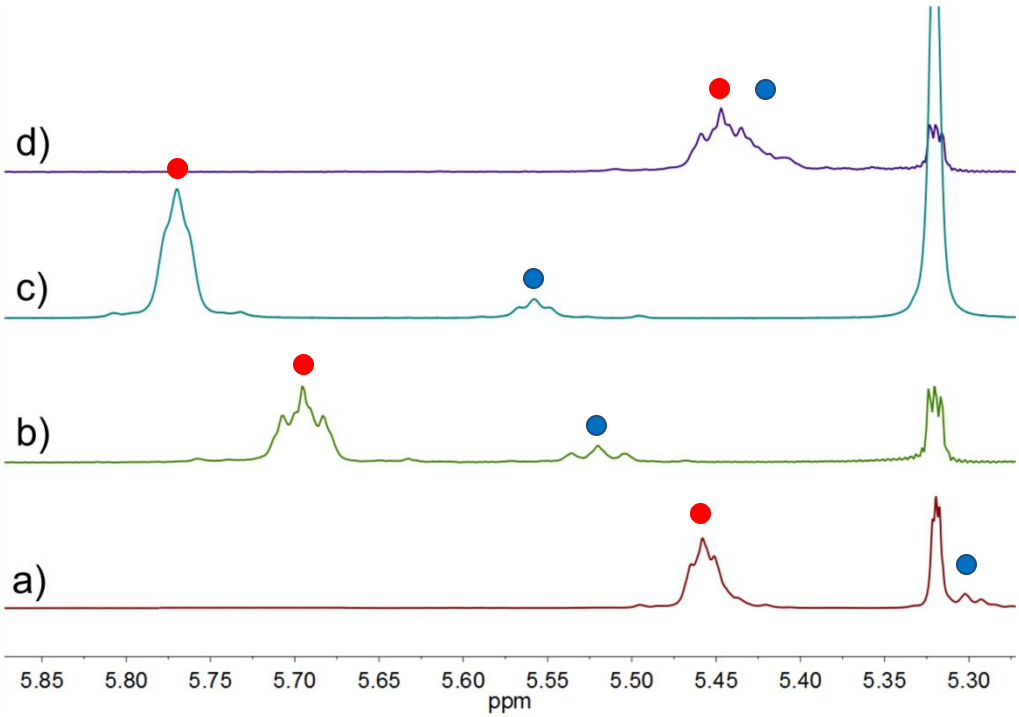

Figure S8. Double bond region (mixture of regioisomers) of ^{1}H NMR spectrum of (a) **3**, (b) **3**•H^+ (trifluoroacetate salt), (c) **3**•Cu^+ (hexafluophosphate salt) and (d) **3**•$(H^+)_2$ (trifluoroacetate salt). CD_2Cl_2, 25 °C.

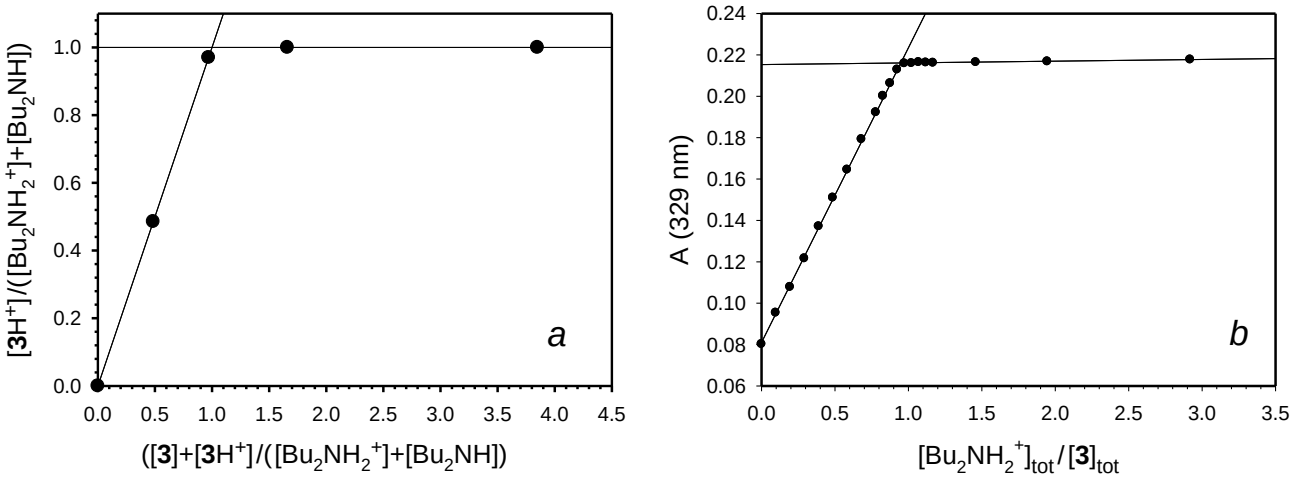

Figure S9. (a) ^{1}H NMR titration of 2.5 mM $Bu_2NH_2PF_6$ with catenand **3** (CD_2Cl_2, 25 °C, see Figure S10). Protonation degree of **3** was measured as a function of the molar equivalents of added **3**. Integrated intensities of the signals of aromatic protons of **3**•H^+ at 8.55 ppm and aromatic protons of **3** at 8.10 ppm (see Figure S10) were followed to produce the plot. (b) UV-vis titration of 0.05 mM catenand **3** with $Bu_2NH_2PF_6$ The quantitative conversion of **3** into **3**•H^+ on addition of 1 molar equivalent of $Bu_2NH_2PF_6$ at concentration as low as 0.05 mM indicates that **3** is more basic than Bu_2NH by at least 5 powers of ten.

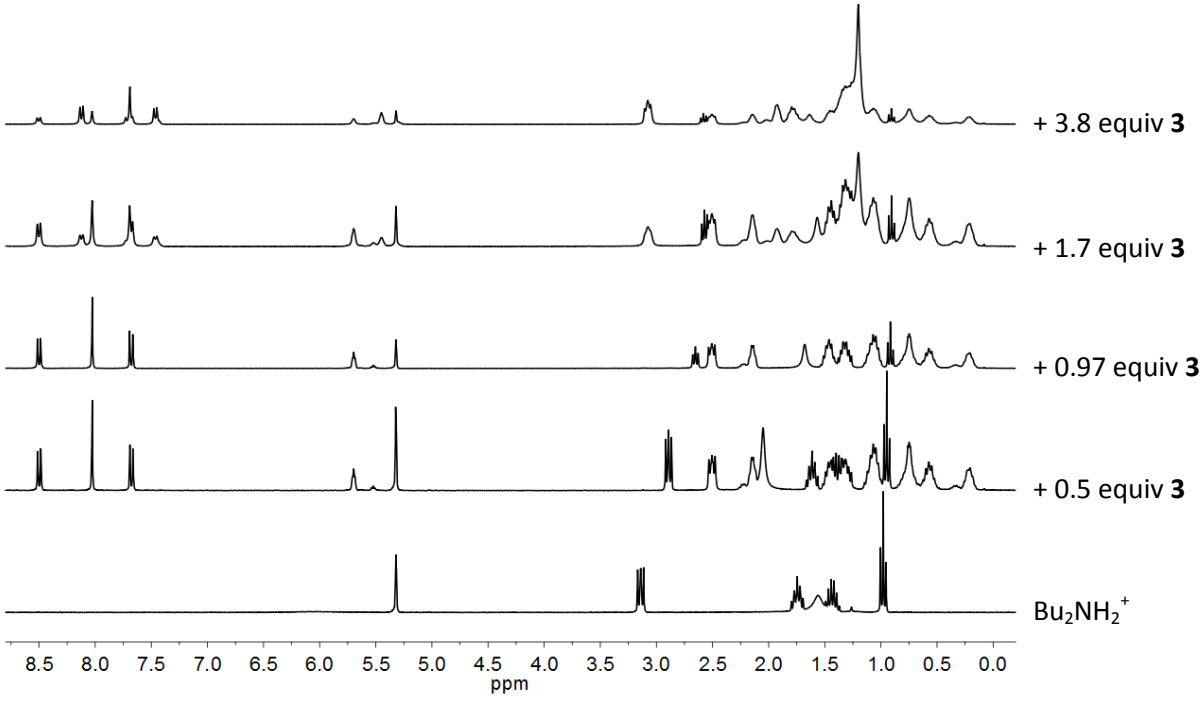

Figure S10.Titration of $Bu_2NH_2PF_6$ (2.5 mM) with **3** in CD_2Cl_2 at 25 °C. Data points in Figure S9 (a) were obtained from these spectra.

*Decarboxylation of acid **1** in the presence of stoichiometric (1:1) and substoichiometric (1:0.5) amounts of Et_3N*

Starting from a mixture of acid **1** and Et_3N[‡] (10 mM each), in CD_2Cl_2 a quantitative conversion into the decarboxylated product **2** was observed in about 5h (Figure S11, *a*). The reaction progress was monitored by ^1H NMR spectroscopy. Typical spectra taken at selected times in the course of reaction are reported in Figure S12. In the presence of ½ molar equivalent of Et_3N (Figure S11, *b*) conversion of **1** to **2** is again quantitative, the reaction rate is lower, and the time-concentration profile has a sigmoid shape typical of autocatalytic reactions. Our interpretation of the observed phenomena in the latter experiment is based on the following scheme, where RCOOH is acid **1** and R-H is reaction product **2**.

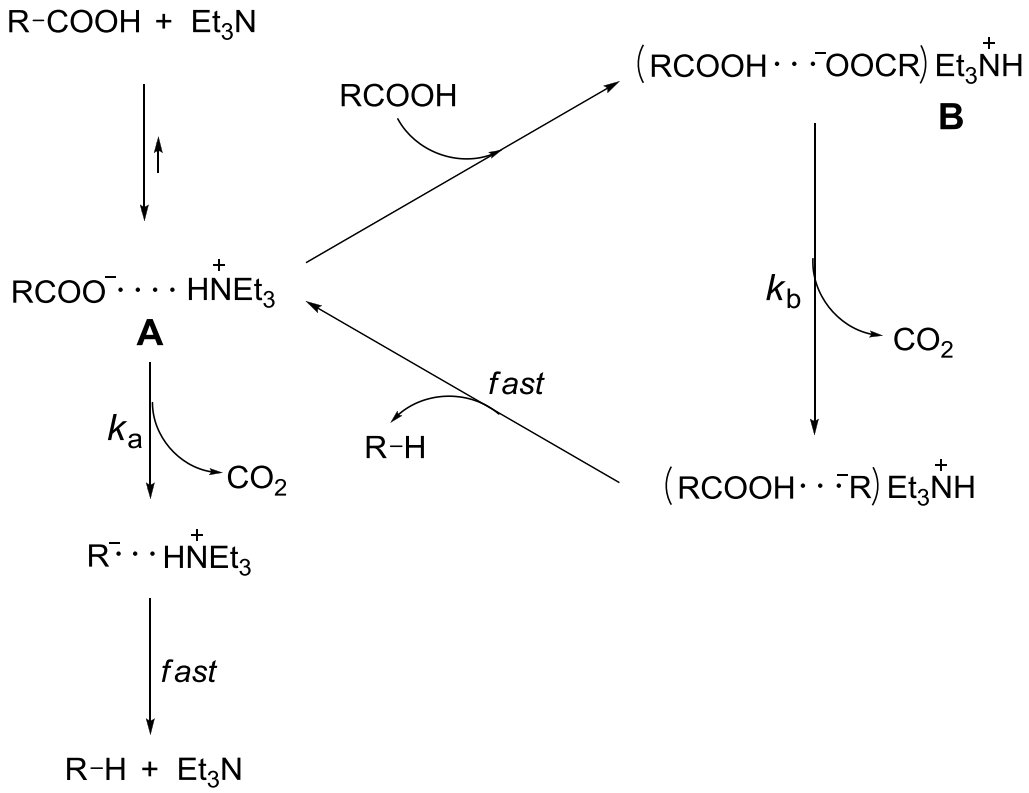

Immediately after mixing the system is a mixture of 5 mM $RCOO^{-}\cdots H\overset{+}{N}Et_3$ (**A**) and 5 mM RCOOH. Since RCOOH is expected to be a much stronger H-bonding donor than $Et_3\overset{+}{N}H$[‡] it

[‡] The pK_a of Et_3NH^+ is 10.76. The pK_a of acid **1** is unknown but it should be not be very different from that of 2-cyanopropanoic acid, pKa = 2.37.

seems most likely that the former favorably competes with the latter for binding to $RCOO^{-}$, thus transforming the ion pair **A** into the ternary adduct **B**.[§] By the same token, the rate of liberation of CO_2 from **B** is expected to be much lower than that from **A** ($k_b << k_a$). In other words, excess acid acts as an inhibitor because transforms the more reactive ion pair **A** into the less reactive ternary adduct **B**. As the reaction proceeds the gradual disappearance of excess acid is paralleled by an increase of the fractional contribution of the more reactive **A** to the overall rate. Thus, the autocatalytic behavior is a consequence of the disappearance of a reactant inhibitor, rather than to the accumulation of a product catalyst.

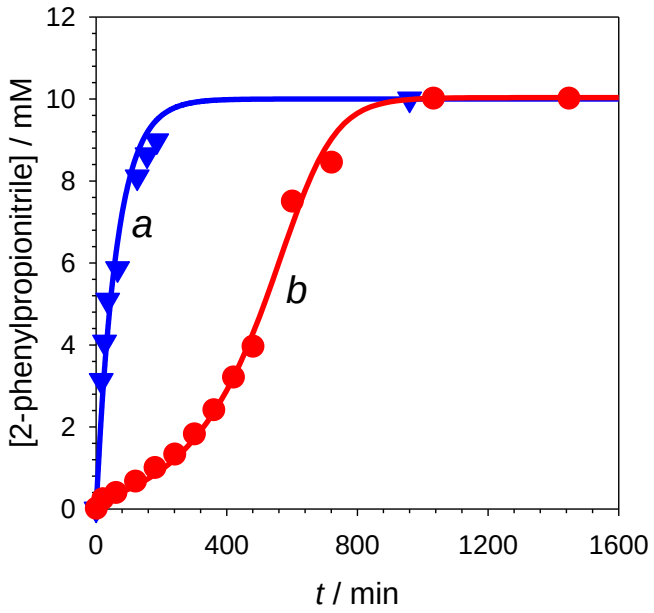

Figure S11. Reaction progress as a function of time for decarboxylation of acid **1** (10 mM) promoted by 1 mol equiv (*a*) and 0.5 mol equiv (*b*) of Et_3N in CD_2Cl_2 at 25 °C. Curve *a* is a plot of a first-order equation. Curve *b* is a guide for the eye.

[§] Because of the low polarity of dichloromethane (ε = 9.08) the concentrations of free ions were assumed to be negligible small.

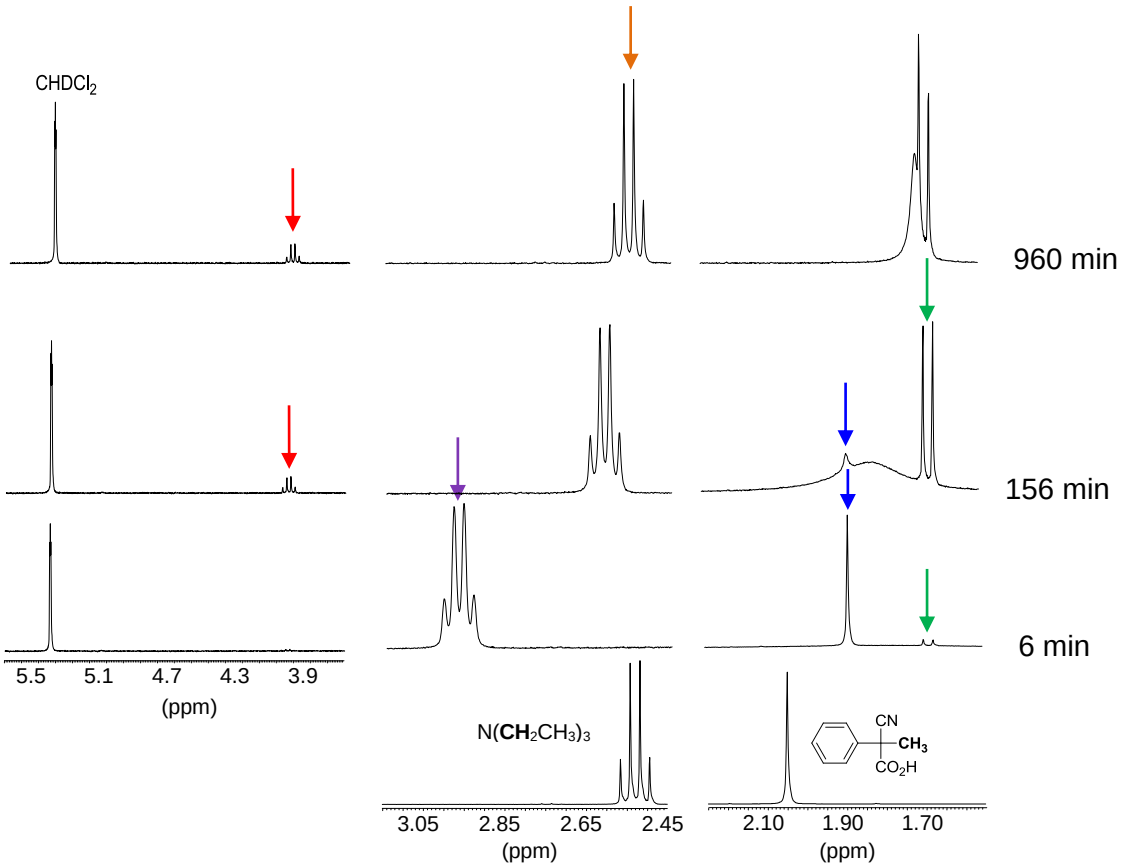

Figure S12. ^{1}H NMR monitoring of the reaction between **1** (10 mM) and Et_3N (10 mM) in CD_2Cl_2 at 25 °C. Typical spectra taken at selected times. Relevant portions of ^{1}H NMR spectra of reactants before mixing are shown for comparison. The broad signal is due to adventitious H_2O. Signals with marks are assigned to the protons with the corresponding color as shown below.

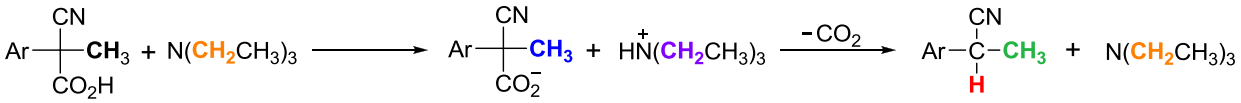

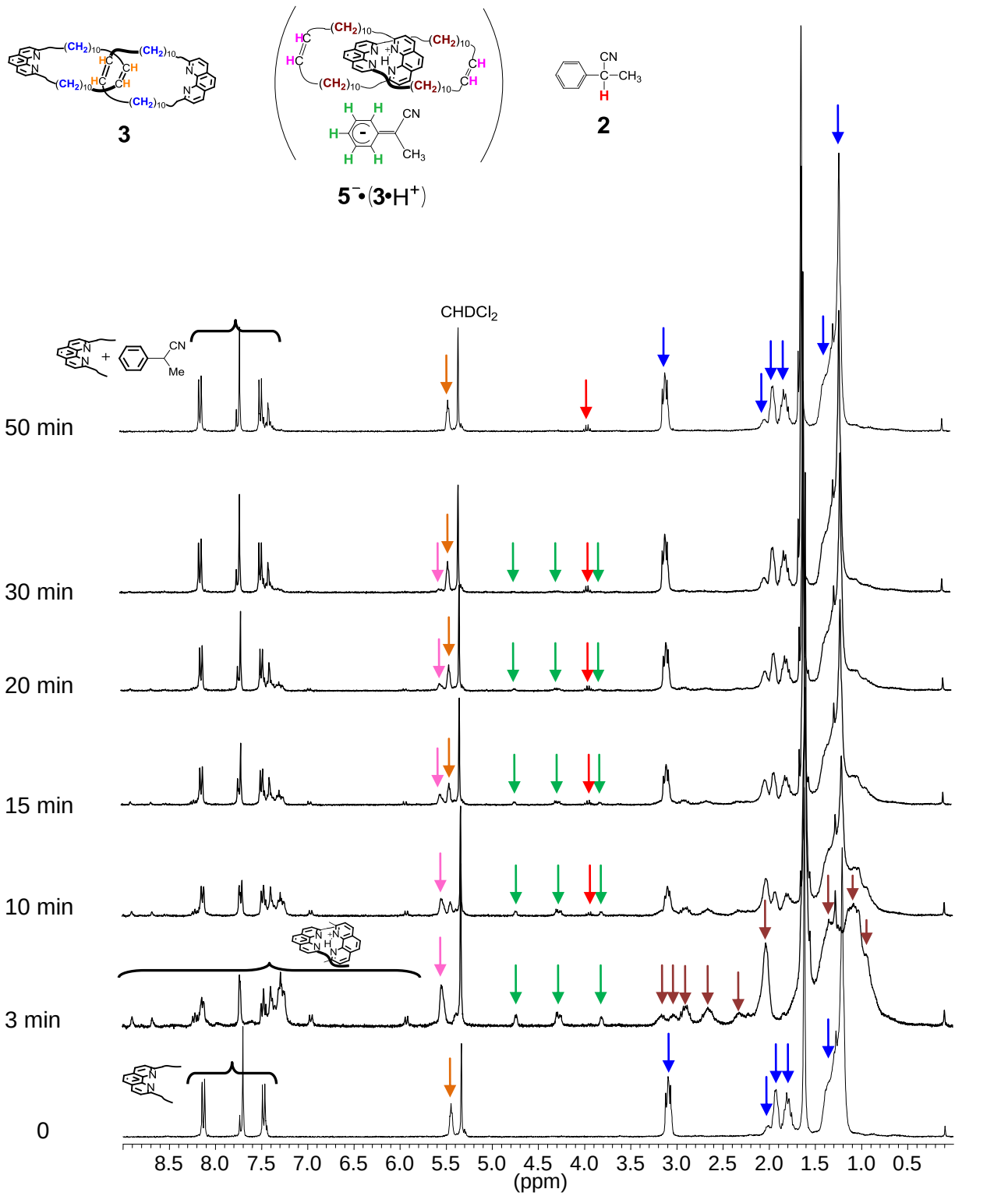

Figure S13. ^{1}H NMR monitoring of the reaction between catenand **3** (5 mM) and acid **1** (5 mM) in CD_2Cl_2 at 25 °C. The trace at time t = 0 is the spectrum of catenand **3**. Signals with marks are assigned to the protons with the corresponding color in the chart at the top of the page.

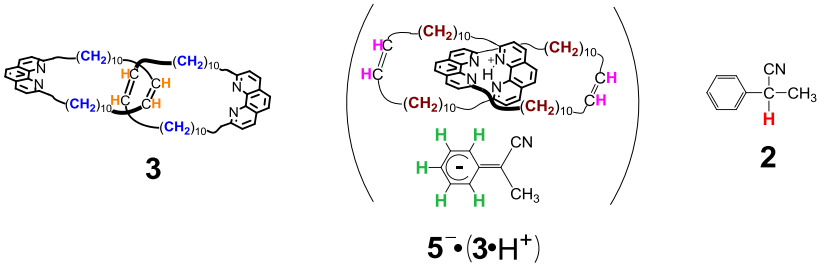

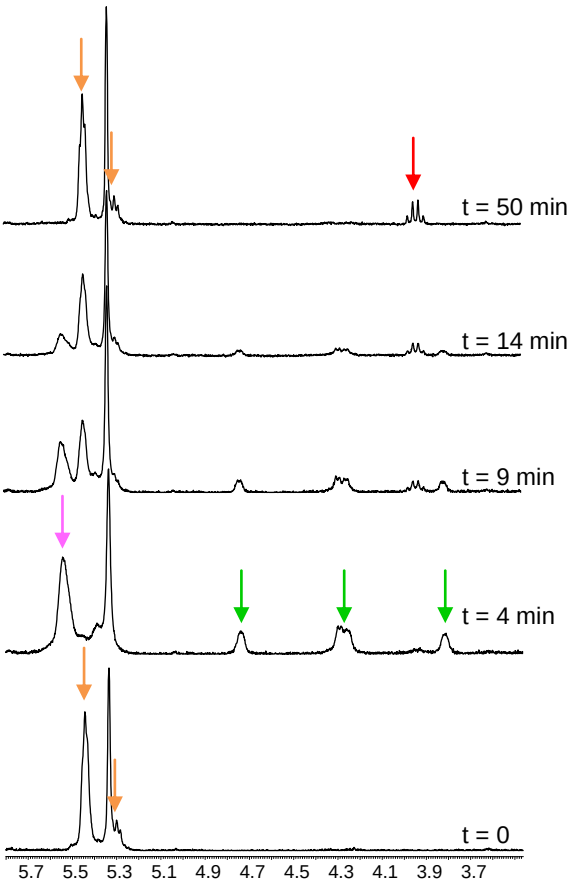

Figure S14. ^{1}H NMR monitoring of the reaction between catenand **3** (10 mM) and acid **1** (10 mM) in CD_2Cl_2 at 25 °C. The trace at time t = 0 is the spectrum of catenand **3**. Signals with marks are assigned to the protons with the corresponding color in the chart at the top of the page.

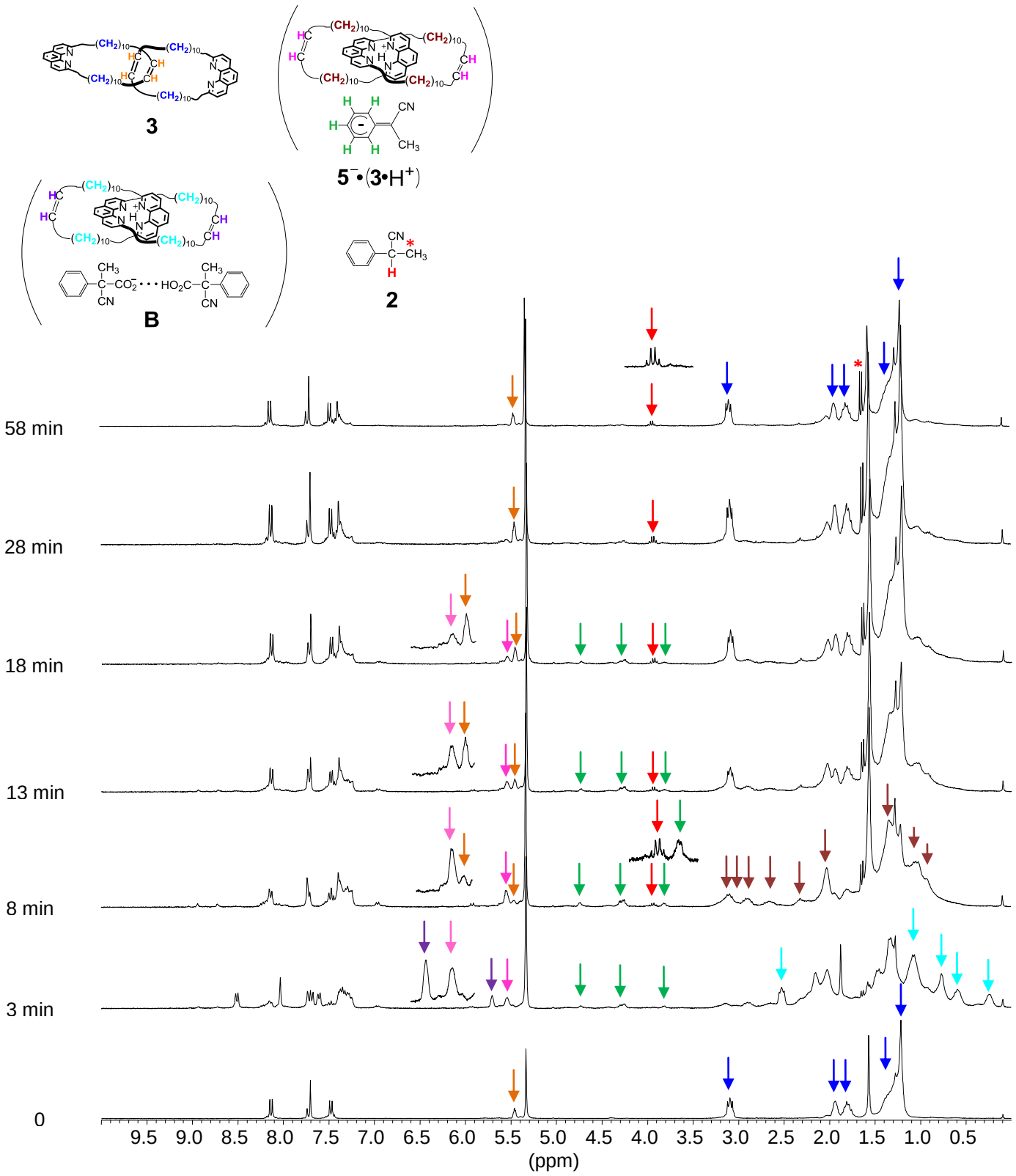

Figure S15. ^{1}H NMR monitoring of the reaction between catenand **3** (2 mM) and acid **1** (4 mM) in CD_2Cl_2 at 25 °C. The trace at time t = 0 is the spectrum of catenand **3**. Signals with marks are assigned to the protons with the corresponding color in the chart at the top of the page. Red asterisk indicates the methyl group doublet of the product.

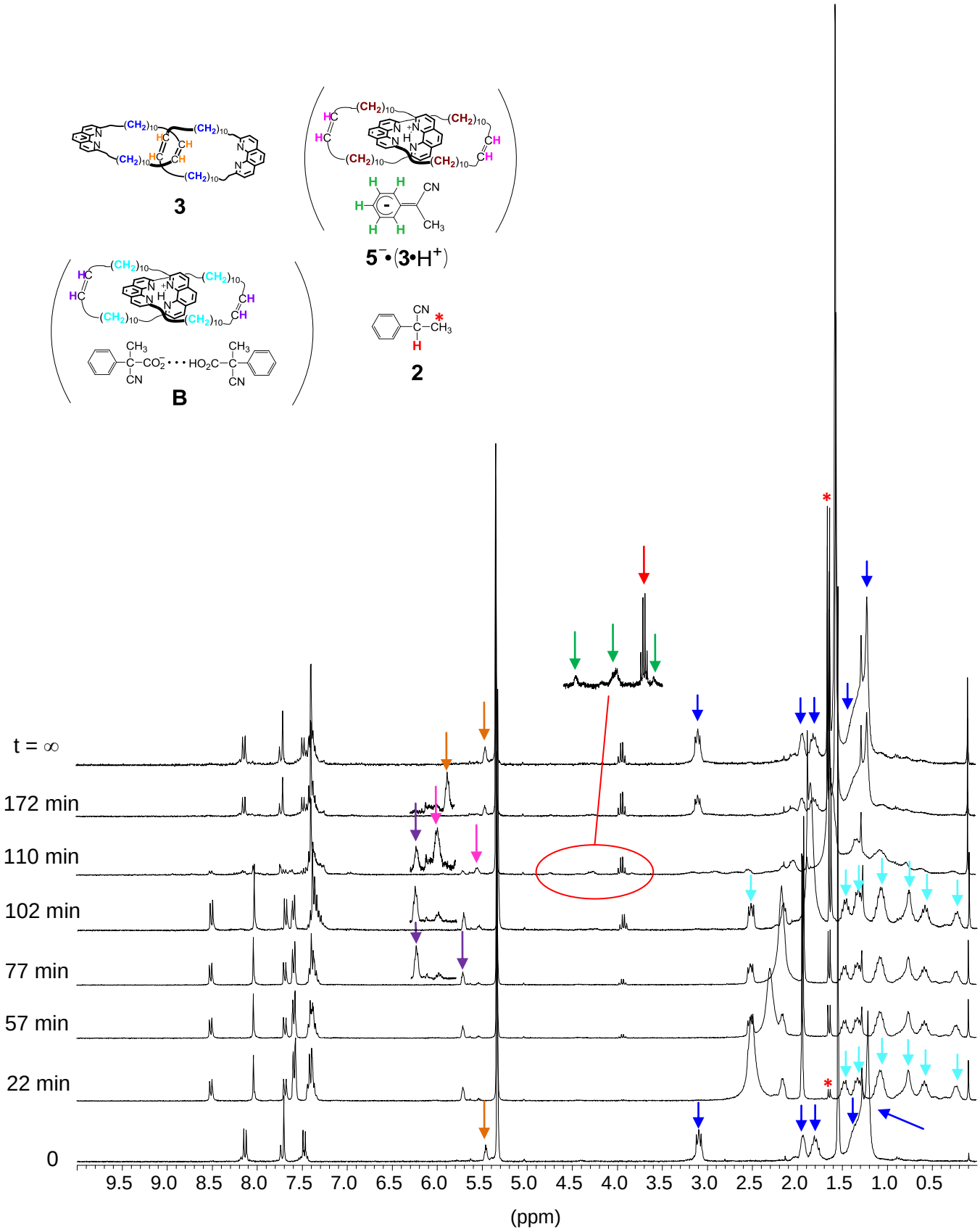

Figure S16. ^{1}H NMR monitoring of the reaction between catenand **3** (0.5 mM) and acid **1** (5 mM) in CD_2Cl_2 at 25 °C. The trace at time t = 0 is the spectrum of catenand **3**. Signals with marks are assigned to the protons with the corresponding color in the chart at the top of the page. Red asterisk indicates the methyl group doublet of the product.